THE JOURNAL OF COMPARATIVE NEUROLOGY 242:381-396 (1985)

The Dorsal Cochlear Nucleus of the Mouse: A Light Microscopic Analysis of Neurons That Project to the Inferior Colliculus

D.K. RYUGO AND F.H. WILLARD
Department of Anatomy and Cellular Biology, Harvard Medical School, Boston, MA 02115 (D.K.R.), Eaton-Peabody Laboratory, Massachusetts Eye and Ear Infirmary, Boston, MA 02114 (D.K.R.), Department of Anatomy, University of New England, Biddeford, ME 04005 (F.H.W.)

ABSTRACT

In the mouse dorsal cochlear nucleus (DCN), all members of a distinct class of large multipolar neurons were shown to project to the contralateral inferior colliculus by using retrograde horseradish peroxidase techniques. Typically, these multipolar neurons have the largest cell bodies in the nucleus and are distributed in layers II, III, and IV. Each contains a round, pale nucleus with a prominent nucleolus and conspicuous Nissl bodies. In Golgi preparations, however, two types of large cells could be distinguished on the basis of dendritic characteristics. Pyramidal cells form relatively flattened, slablike dendritic fields whose alignment contributes to the laminar organization of the DCN. They represent 75–80% of the large cell population and are found in layer II and the superficial region of layer III. Giant cells represent the other type of large multipolar neuron and are distributed in the deeper regions of layer III and in layer IV. Their ellipsoidal dendritic fields are formed by long and relatively unbranched dendrites that project across the laminae. The differences in dendritic morphology imply that each cell class segregates its afferent input in distinct ways and subserves different auditory functions.

Key words: auditory system, giant cells, horseradish peroxidase, pyramidal cells

The cochlear nucleus receives incoming auditory nerve discharges and distributes the output signals to higher centers in the brain. The output projections of the cochlear nucleus are organized according to specific cell types and segregate into separate pathways (Harrison and Feldman, '70; Ryugo et al., '81; Cant, '82; Tolbert et al., '82; Adams, '83). Some of the cell types have been associated with certain discharge characteristics and postsynaptic targets (e.g., Kiang, '75; Tsuchitani, '78; Cant and Morest, '84). The resulting circuits establish "wiring diagrams" that are key to understanding how acoustic information is spatially and temporally processed within the central nervous system. In this context, we have been studying the neural circuitry of the cochlear nucleus.

The dorsal cochlear nucleus (DCN) of nonprimate mammals is a cortical structure containing a number of cell types organized into four distinct layers (Ramón y Cajal, '09; Brawer et al., '74; Lorente de Nó, '81; Mugnaini et al., '80; Willard and Ryugo, '81; Webster and Trune, '82). On the basis of studies that used the retrograde transport of horseradish peroxidase (HRP), some of these DCN neurons have been shown to project to the contralateral inferior colliculus (Ryugo et al., '81). Specifically, when injections of HRP were restricted to either the central nucleus or the external cortex of the inferior colliculus, large multipolar neurons were labelled in the contralateral DCN. The labelled neurons were arranged in "sheets" that spanned layers II–IV and were topographically related to the injection sites in the inferior colliculus. Only the largest neurons of the DCN contained the HRP label, although unlabelled neurons of equal size were intermixed with labelled ones. These observations raised the issue as to whether the unlabelled large neurons possessed connections with different regions of the brainstem, or whether they simply had inadequate access to the injected HRP. The large multipolar

Accepted August 16, 1985.

Address reprint requests to Dr. D.K. Ryugo, Department of Anatomy and Cellular Biology, Harvard Medical School, 25 Shattuck Street, Boston, MA 02115.

neurons were similar to one another with respect to their perikaryal size and cytological features but were dissimilar with respect to perikaryal shape, orientation, and/or position with respect to cortical layer. Thus, a second issue arose, which was how to organize neurons that were similar in many respects, yet different in others.

This report addresses anatomical features that provide reliable indicators for distinguishing subgroups of neurons in the mouse DCN. Cells projecting to the midbrain were labelled following HRP injections into the inferior colliculus. This neuronal population represents one link in a neural circuit, and retrograde labelling forms the basis for grouping cells having different characteristics. Certain other morphological features of these cells were sufficiently distinct that the population could still be recognized in mice whose cochlear nuclei were prepared by different histological procedures. Two classes of midbrain-projecting neurons have been distinguished on the basis of dendritic form and relative position (depth) in the nucleus.

MATERIALS AND METHODS

Subjects

Young adult mice (20–25 g) of either sex were obtained from the Charles River Breeding Laboratories, Wilmington, MA. The data for the present study have come from albino ICR and CD-1 mouse strains, and all basic observations have been verified in a pigmented strain (C57BL/6).

Histological procedures

The light microscopic descriptions of the DCN and its constituent cells are based on Nissl, protargol, and Golgi staining techniques that have been previously described (Bodian, '36; Ryugo and Fekete, '82; Willard and Ryugo, '83). DCN neurons were labelled using HRP methods. Briefly, animals were anesthetized with 3.5% chloral hydrate (1 cc/100 g body weight), mounted on a stereotaxic apparatus, and the calvaria overlying the midbrain were surgically removed. A unilateral pressure injection of 30% HRP in 0.1 M Tris buffer was delivered to the inferior colliculus (IC) with a stereotaxically mounted microsyringe (rate = 0.5 μl/10 minute). After a survival period of approximately 24 hours, the animals were deeply anesthetized and perfused through the heart with 0.1 M phosphate-buffered saline (25 ml, pH 7.2) followed by 250 ml of fixative (0.1 M phosphate buffer, 2.5% glutaraldehyde, 1.25% paraformaldehyde, pH 7.2). The heads were postfixed for 6 hours, and the brains were then removed and stored overnight in the same fixative plus 10% sucrose (w/v) at 5°C. The next day, the brains were transferred to a solution of 30% sucrose in 0.1 M phosphate buffer (pH 7.2). After the brains sank to the bottom of the solution (within 24 hours), frozen coronal or sagittal sections (50 μm thick) were collected, serially mounted on "subbed" slides, and processed using benzidine dihydrochloride (Mesulam, '76), tetramethylbenzidine (Mesulam, '78), or diaminobenzidine (Adams, '77). Treated sections were lightly counterstained with a 0.5% cresyl violet solution, dehydrated, and coverslipped with Permount.

Data analysis

A coronal atlas for each cochlear nucleus used in this study was prepared in 10% intervals. Percentages were determined by dividing the section number by the total number of sections per nucleus (e.g., Ryugo et al., '81). By use of a light microscope and drawing tube attachment, the boundary of the DCN was outlined at a total magnification of ×312, vascular landmarks were drawn, and an "x" was placed over the nucleus of each labelled cell. A second drawing of each section was made that included only vascular landmarks and the boundaries of the cortical layers. The two drawings were then superimposed by using the vascular landmarks so that the laminar position of each cell body could be determined.

Individual cells were studied at a total magnification of ×1,250. Drawing tube reconstructions of cells were also performed at a total magnification of ×1,250. In order to standardize our sampling procedure for comparisons across Nissl, Golgi, and HRP techniques, only neurons located near the 50th percentile through the coronal atlas were used for morphometry. Analysis was performed on all labelled cells exhibiting cytoplasmic HRP granules and all unlabelled cells exhibiting cytoplasmic Nissl substance, a clear nuclear envelope, and a nucleolus. In the present study, Nissl bodies are defined as clumps of Nissl substance having any dimension greater than 1 μm. The method of establishing cell body perimeter was standardized by placing a line across the silhouette of each neuron where paired concavities were formed between the cell body and the stalks of each primary dendrite. The perimeter of each silhouette was then traced onto a computerized planimeter, and area and short/long axis ratio were determined for each cell body. There was no attempt to "correct" these measurements for differential shrinkage between the various histological preparations or across animals.

RESULTS

The cochlear nucleus was recognized as a lateral protrusion from the brainstem surface at the pontine-medullary junction (Fig. 1). The external boundary between the dorsal and ventral nuclei was marked by a shallow, curved depression along the lateral surface of the nucleus. The DCN extended dorsomedially from its broader base overlying the VCN and wrapped around the caudolateral aspect of the inferior cerebellar peduncle; in this way, the dorsomedial apex of the nucleus approaches the lateral wall of the fourth ventricle. The long axis of the nucleus extended from the dorsomedial apex to the ventrolateral base (called the "strial axis" by Blackstad et al., '84). The short (or "trans-strial") axes were oriented perpendicular to the surface of the nucleus and to the long axis, and coincided with the "sheets" of neurons that projected to restricted laminae in the contralateral inferior colliculus (Ryugo et al., '81).

Cytoarchitecture and cell layers

The separate layers of the mouse DCN were distinguished on the basis of relative cell density (Fig. 2A), differing proportions of the various cell types (Fig. 2B), and the texture of the neuropil (Fig. 2C). Layer I was relatively cell sparse and of uniform thickness. It bordered the pial surface of the DCN. Layer II was also of uniform thickness but was characterized by a high density of granule cells and large multipolar neurons. Layer III was characterized by a reduction in cell density compared to that of layer II; it has been called the deep polymorphic layer due to the variety of cell types contained within. Terminal ramifications of auditory nerve fibers were also contained within this layer. Layer IV encompassed the dorsal acoustic stria lying at the base of the DCN. This layer was characterized by a high density of glial cells that aligned along the fascicles of strial fibers. The boundary between layer III and IV was evident

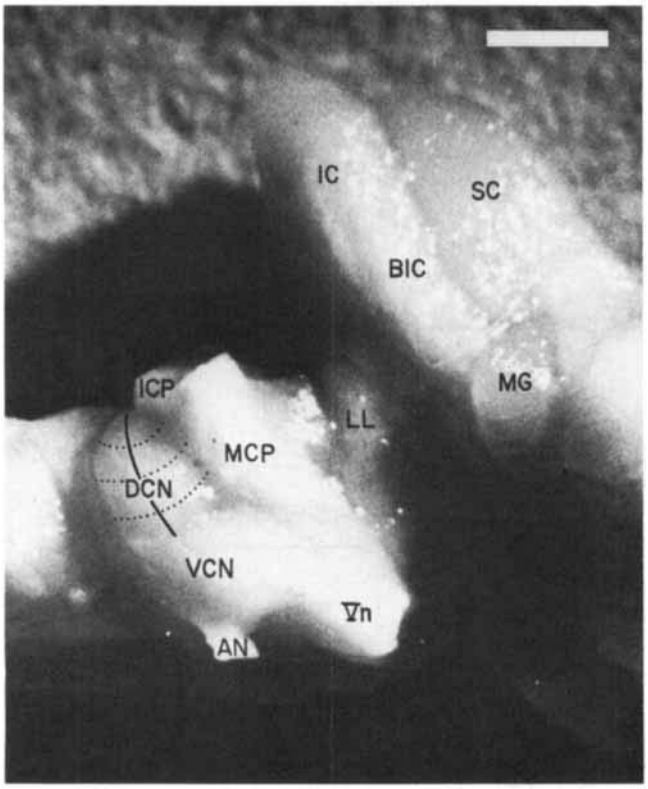

Fig. 1. Photograph of right cochlear nucleus of the mouse (lateral view). The long axis of the nucleus is indicated by the thin solid line. Several of the short axes are indicated by the dotted lines. The DCN may be imagined as a loaf of sliced bread, where each "slice" represents an isofrequency slab as well as a sheet of midbrain-projecting cells. Dorsal is up, anterior is to the right. Abbreviations: AN, auditory nerve; BIC, brachium of inferior colliculus; DCN, dorsal cochlear nucleus; IC, inferior colliculus; ICP, inferior cerebellar peduncle; LL, lateral lemniscus; MCP, middle cerebellar peduncle; MG, medial geniculate nucleus; SC, superior colliculus; VCN, ventral cochlear nucleus; Vn, trigeminal nerve root. Scale bar equals 1 mm.

in that a 90° shift in the orientation of cell bodies and fibers occurred at this interface.

In summary, layers I and II formed a blanket of uniform thickness that covered layer III. Layer III was shaped like an elongated teardrop whose medial surface was flattened against the convexity of layer IV; layer III was narrow at its dorsomedial apex and broad at the ventrolateral base. These layers have been mapped into coronal and sagittal sections to create an atlas of the mouse DCN (Fig. 3).

Cytoarchitecture and cell laminae

Orthogonal to the DCN layers, cells within layers II and III were arranged in parallel sheets that spanned the short axis of the nucleus. In stained histological sections (taken approximately parallel to the long axis of the DCN), these sheets appeared as rows of cells (Fig. 4). The rows were further emphasized by the elongated perikaryal profile of most large multipolar neurons. We will introduce the term "lamina" in reference to these apparently repeating sheets of cells; in contrast, the term "layer" is used when referring to the nonrepeating cortical structure of the DCN. The cellular laminae also correspond to the parallel contours defined by afferents from the cochlea (unpublished observations).

Cytoarchitecture and cell types

Based on Nissl-stained material, four general classes of neurons (excluding glial and granule cells) were distinguished. Large multipolar neurons represented the most salient cell class in the DCN and were distributed across layers II–IV (Fig. 5A). These neurons characteristically had two to six primary dendrites, a relatively large cell body, and a pale-staining, centrally located nucleus. Their cytoplasm stained lightly but contained dark-staining, coarse, granular Nissl substance and many conspicuous Nissl bodies (Fig. 6A–L). On the basis of these features, every cell in the DCN was classified as either "large multipolar" or "other," a distinction that was highly predictive of cell body

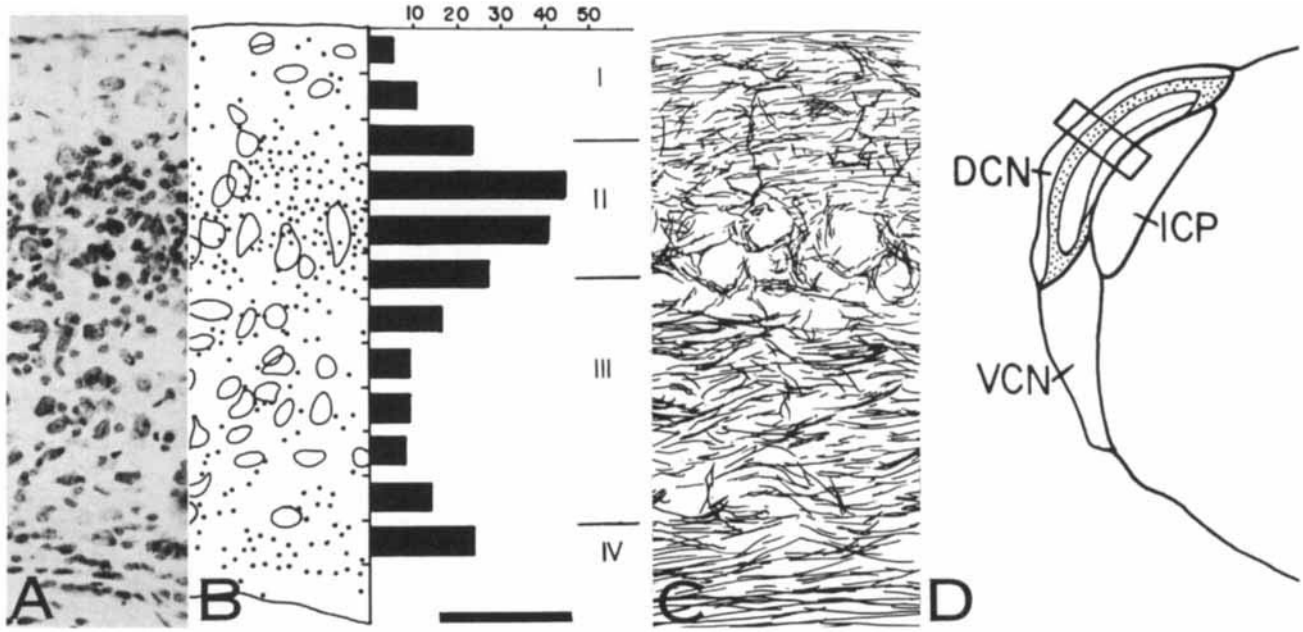

Fig. 2. Characteristics of DCN layers. A. Photomicrograph of a 15-μm-thick, Nissl-stained, coronal section through the middle of the DCN. B. Drawing tube reconstruction of A, illustrating macroneurons (open profiles) and glial and granule cells (solid dots). The DCN has been divided into vertical bins, each 25 μm deep. The total number of glial and granule cells in each bin is depicted by the bars in the accompanying histogram. Variations in density of glia and granule cells coincide with the layer boundaries (where histogram peaks fall between 20 and 30 cells/bin). Scale bar for A, B, and C equals 75 μm. C. Drawing tube reconstruction of a 15-μm-thick, protargol-stained section immediately adjacent to the section illustrated in panel A. Note how the texture of the neuropil changes according to DCN layer. D. Schematic diagram of brainstem where boxed area indicates regions presented in A–C. Abbreviations are the same as in Figure 1.

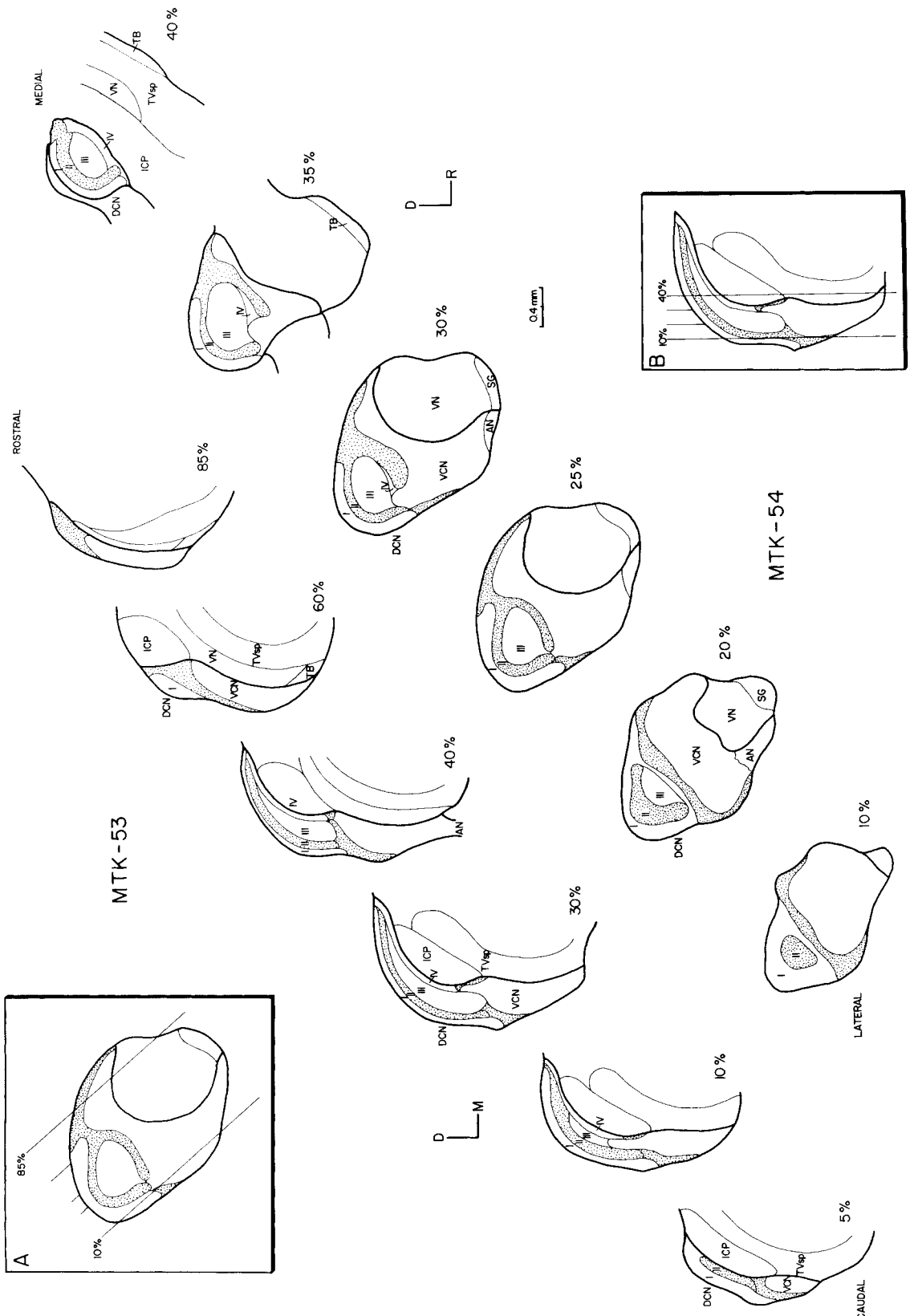

Fig. 3. The distribution of layers in the DCN is illustrated in coronal (MTK-53) and parasagittal (MTK-54) atlases. The granule cell zones have been indicated by stippling. Inset A orients the plane of section for MTK-53; inset B orients the plane of section for MTK-54. Abbreviations: D, dorsal; R, rostral; SG, Scarpa's ganglion; TB, trapezoid body; TVsp, descending tract of the trigeminal nerve; see also Figure 1.

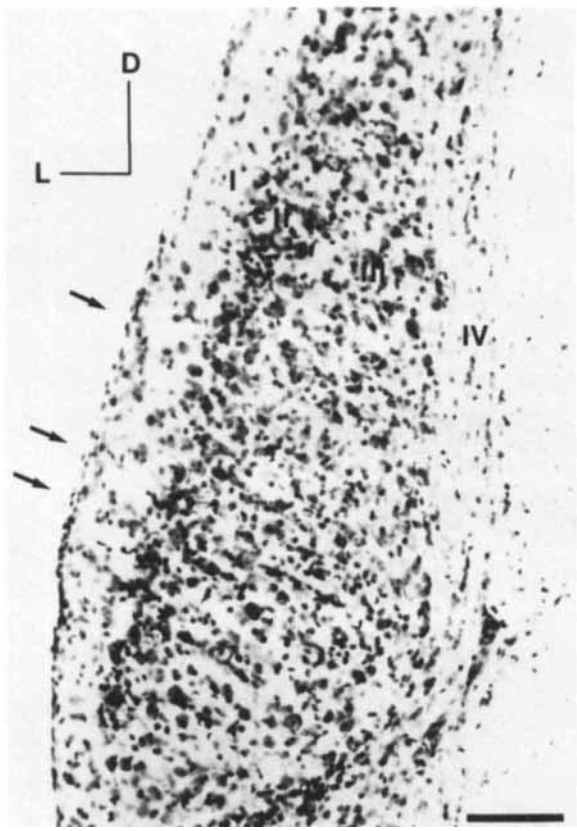

Fig. 4. Photomicrograph of a 40-μm-thick, vibratomed, Nissl-stained coronal section. The plane of this section approximates the 40th percentile (see MTK-53 inset, Fig. 3). Note the cell striations that generate what we have called "laminae" (arrows). The laminae are oriented roughly perpendicular to the cortical layers (I–IV). Abbreviations: D, dorsal; L, lateral. Scale bar equals 0.1 mm.

size (Fig. 7). Within the group of large multipolar neurons, however, silhouette areas were not a reliable predictor for cell body position according to cortical layer. The large multipolar neurons in layers II and III were virtually indistinguishable from one another in Nissl-stained material. The cell bodies of these neurons typically had their long axes oriented perpendicular to the DCN surface (Fig. 5A), although individual neurons could vary considerably in shape and orientation (Fig. 6A–H). In the middle regions of layer III, these neurons tended to be more symmetrical and stellate in appearance. In the deep regions of layer III and in layer IV, the large multipolar neurons were oriented at right angles to many of those in layers II and III. That is, they were elongated parallel to the strial fibers and parallel to the long axis of the nucleus. These neurons exhibited cytological features typical of the large multipolar neurons of layers II and III (Fig. 6I–L).

A second major class of neurons (prominent in layers I and II) was composed of "round cells" (Fig. 5B). They had spherical perikarya, a centrally placed nucleus, and a single prominent nucleolus. Surrounding the nucleus was a band of cytoplasm containing lightly staining, fine granular Nissl substance (Fig. 6M,N). Based on similarities in perikaryal shape, size, and location, these neurons correspond to what have been called cartwheel cells (Brawer et al., '74; Webster and Trune, '82; Wouterlood and Mugnaini, '84).

The remaining constituents of the DCN have been lumped into the general category of "small multipolar cells" (Fig. 5C). This cell group was heterogeneous, and at least two subtypes were routinely identified. The most common of the small multipolar cells composed the third major class of neurons and they were found throughout all the layers; these are the "light-staining, small multipolar neurons." Their cell bodies had an irregular contour and contained an oval, pale-staining nucleus with multiple clumps of heterochromatin. A thin rim of cytoplasm characterized by lightly staining Nissl substance surrounded the nucleus, (Fig. 6O,P). The fourth general class of neuron was the "dark-staining, small multipolar neuron." These cells were encountered less frequently and primarily in layer III; they were characterized by intensely staining cytoplasmic Nissl substance (Fig. 6P,Q).

DCN neurons that project to the inferior colliculus

Midbrain-projecting neurons of the DCN were retrogradely labelled following unilateral pressure injections (1–3 μl) of HRP into the IC. For cases (n = 5) where the injection site was localized to the entire IC and surrounding fringe of tissue, all of the larger neurons in the contralateral DCN contained the HRP reaction product; the smaller neurons did not (Fig. 8). This characteristic size difference between labelled (filled circles) and unlabelled neurons (open circles) is illustrated in Figure 9.

The relative distribution of labelled cells through the DCN was determined according to layers and found to be similar for both large and discrete injections of HRP into the IC and corresponded to the distribution of large multipolar neurons as determined by cytological criteria (Table 1). It should be noted that the absolute number of large multipolar neurons did vary from animal to animal even within the same strain and age of mice.

The combined shape of cell body and proximal dendrites resulted in a relatively flattened appearance of the labelled cells within layer II and the superficial regions of layer III. This flattened profile was quite evident throughout the nucleus (especially in selected sections where the cells are optimally viewed "on edge"). The height and shape of labelled cells (when viewed perpendicular to the long axis of the nucleus) varied within the DCN. In the dorsomedial region of the DCN, labelled cells were relatively short and stocky; they became progressively taller and thinner toward the ventrolateral base of the nucleus (Fig. 10).

The absolute axis of orientation for labelled neurons also varied systematically as a function of position within the nucleus (Fig. 10), presumably because the DCN curves over the convexity of the brainstem. The dorsomedial region of the DCN contained short neurons that tended to be oriented vertically in the coronal plane (Fig. 10A), and were viewed *en face* in the parasagittal plane (Fig. 11C,D). In the more lateral regions of the DCN, neurons tended to have a horizontal orientation in the coronal plane (Fig. 10B), and were viewed from their apical edge in the parasagittal plane (Fig. 11A,B). In the ventrolateral base of the DCN, neuronal orientation was rotated past horizontal (Fig. 10C), and cells in this region still appeared thin and spindle shaped when viewed in the parasagittal plane (Fig. 11A,B).

Golgi analysis

Horseradish-peroxidase- and Nissl-stained material revealed anatomical features of cell bodies and the proximal dendritic stumps of the large multipolar neurons. A more

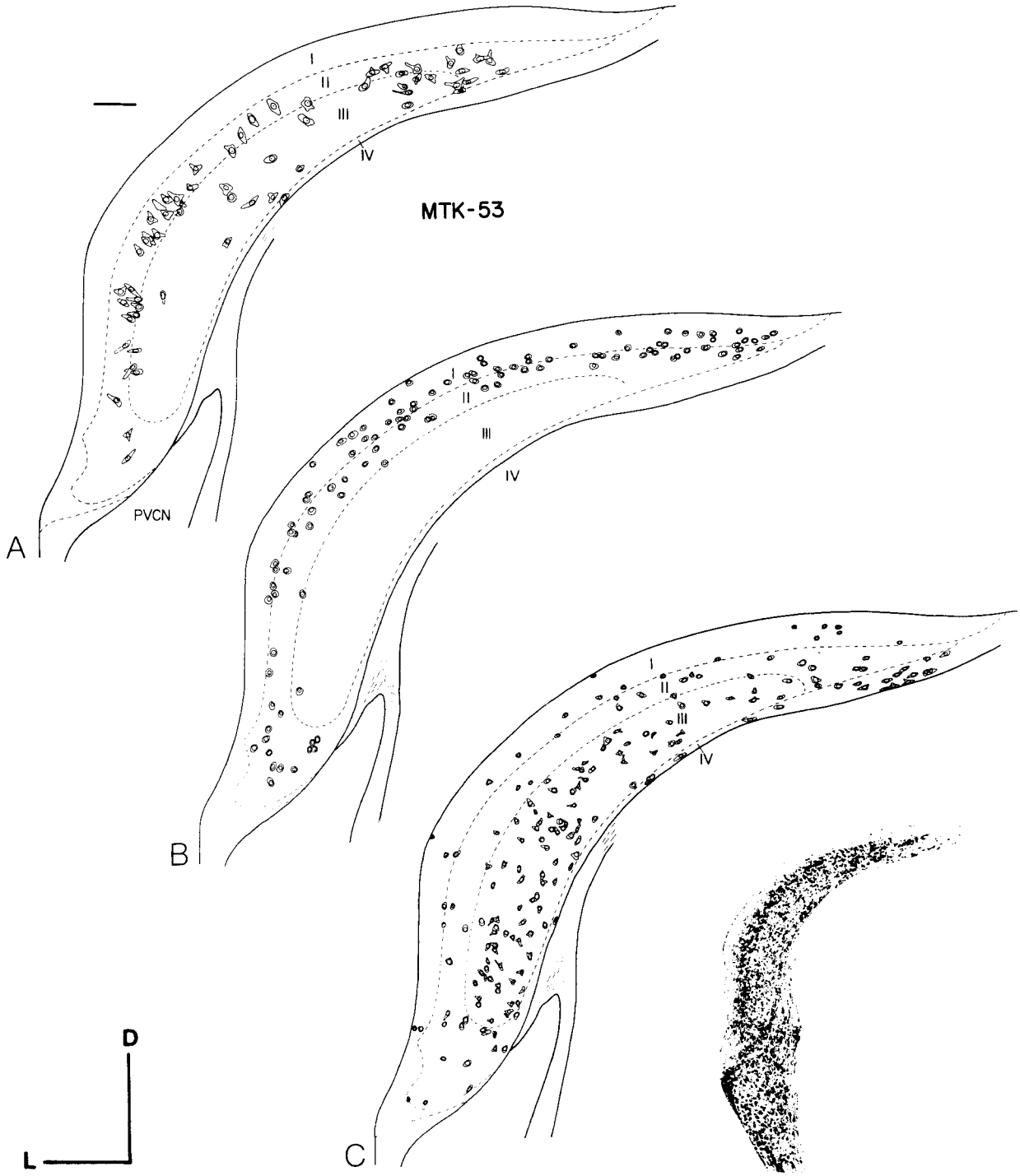

Fig. 5. Drawing tube reconstruction of stained section (shown in inset) illustrating the distribution of identifiable cell types in the DCN. A. Distribution of large multipolar neurons. B. Distribution of round (cartwheel) cells. C. Distribution of small multipolar neurons. Inset: Photomicrograph of a 15-μm-thick Nissl-stained coronal section through the 50th percentile of the DCN. Abbreviations: D, dorsal; L, lateral; PVCN, posteroventral cochlear nucleus. Scale bar equals 0.1 mm.

detailed study of dendritic characteristics was accomplished using Golgi methods. On the basis of results presented in Figures 7 and 9, it appears that perikaryal size is sufficient for identifying most of the large multipolar neurons in Golgi preparations. This size distinction was of practical importance because the Golgi precipitate obscured cytoplasmic Nissl patterns and other staining characteristics. We deliberately selected those Golgi-impregnated neurons residing in layers II–IV and having a cell body area that exceeded 250 μm^2, in order to have confidence that only large multipolar neurons were included in the analysis. The shapes of Golgi-impregnated cell bodies shared similarities with those of the large multipolar neurons revealed by other histological techniques, and within layer II, a gra-

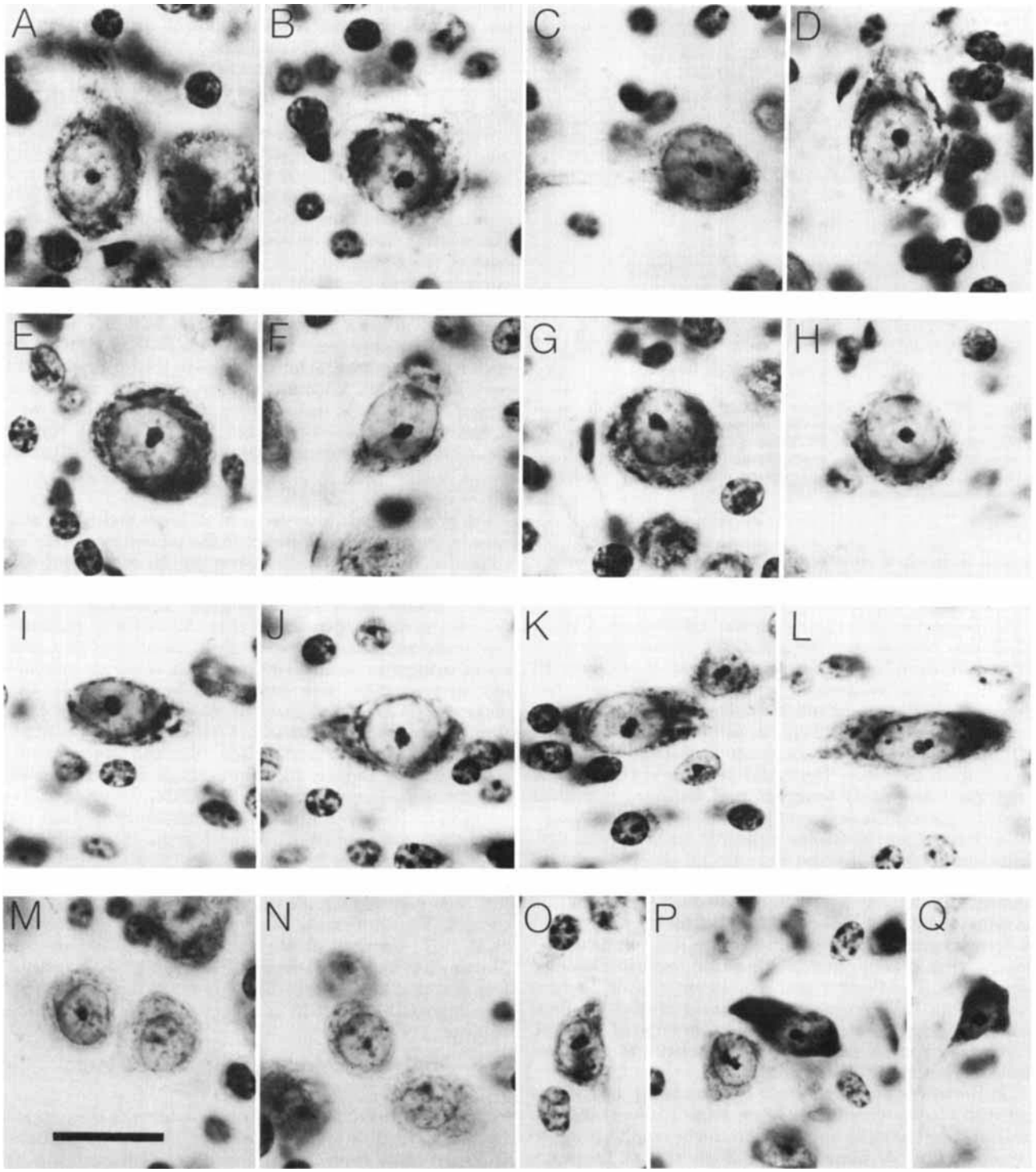

Fig. 6. Photomicrographs of representative cell types in the DCN as seen in Nissl-stained sections. Large multipolar neurons are shown for layer II (A–D), layer III (E–H), and layer IV (I–L). Note the cytological similarities among members of this group. Examples are also shown of round (cartwheel) cells found in layer I (M,N) and of small multipolar cells of layer III (light, O,P; dark, P,Q). Ependymal surface is toward the top of the page. Scale bar for all photographs equals 20 μm.

dient in neuronal height, orientation, and dendritic arbor width was noted (Fig. 12). The change in apparent width represented a sectioning artifact created by the progressive and systematic change in orientation of the flattened dendritic fields of these neurons and was related to cochleotopic position in the nucleus. The plane of these flattened arbors seemed to remain constant relative to the trajectory of eighth nerve axons. In order to maintain alignment with these primary axons (whose trajectory gradually changes), the dendritic fields also rotate. Thus, dendritic trees ap-

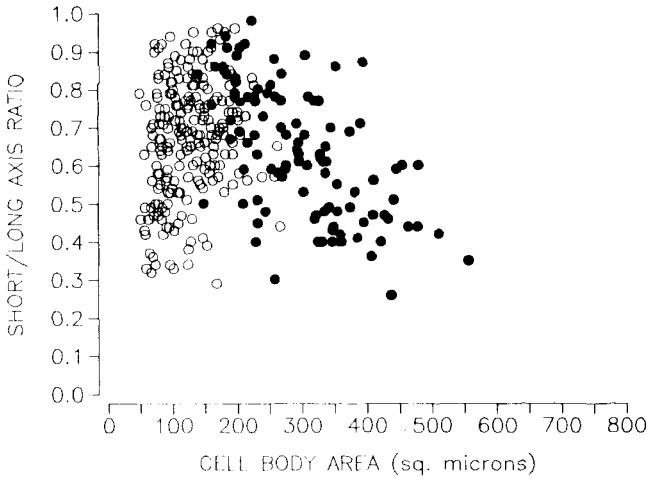

Fig. 7. Plot of cell body silhouette area and short/long axis ratio for all neurons in three alternate 15-μm-thick sections spanning the 50th percentile through the nucleus (MTK-53). Filled symbols represent neurons with prominent Nissl bodies; open symbols represent neurons with no Nissl bodies. Note how neurons having prominent Nissl bodies tend to have the largest cell body silhouette area.

peared thin when viewed on edge in the ventrolateral region of the nucleus and appeared "fat" when viewed more *en face* in the dorsomedial region.

The population of large multipolar neurons could be divided into two groups. The perikarya of one group were located in layer II and the superficial regions of layer III (Fig. 13). These neurons, a type of pyramidal cell, had substantially flattened dendritic fields. Typically, two to six primary dendrites arose from the cell body. One or several of these dendrites were directed into layer I and formed the apical dendritic arbor. The distal portions of these apical dendrites were highly branched and displayed numerous dendritic spines; the proximal portions of these apical dendrites tended not to display dendritic spines. Basal dendritic arbors were formed by one or several primary dendrites directed into layer III. These basal dendrites coursed for relatively long distances without branching and terminated by ending blindly or by branching a few times to form a small tuft. Dendritic spines are conspicuously absent. Occasionally, laterally directed dendrites coursed along layer II and either branched to enter layer I, where they assumed the morphological characteristics of apical dendrites (highly branched and spiny), or entered layer III, where they conformed to the characteristics of the basal dendrites (unbranched and nonspiny).

The flattened dendritic domains of pyramidal cells (where individual cells were viewed "on edge") intersected the cortical layers at right angles and could be readily observed in coronal and horizontal sections (Figs. 12, 13). The orientation of these flattened domains corresponded to the cellular laminae observed in Nissl-stained material. Within these more-or-less two-dimensional domains (corresponding to the short axis planes of the nucleus), the dendrites radiated broadly. An *en face* view of three pyramidal cells is illustrated in Figure 14.

Giant cells were the other type of large multipolar neuron and their irregularly shaped cell bodies were scattered in the deeper regions of layer III and in layer IV. These neurons were characterized by long (up to 1 mm) and relatively unbranched dendrites that extended in many directions. The relative size of these neurons with respect to the thickness of the tissue sections (80–200 μm) meant that to a varying degree the distal portions of some dendrites were lost. Nevertheless, by studying tissue sectioned in different orientation planes, it was determined that the dendritic fields of giant cells could invade layers II–IV, and that each field had its greatest extent parallel to the long axis of the nucleus (Fig. 15). Within this large field, the distal dendrites of giant cells tended to be aligned with basal dendrites of pyramidal cells, and this alignment further contributed to the laminar appearance of the DCN (Fig. 13).

DISCUSSION

The present study revealed that all large multipolar neurons in the mouse DCN project to the contralateral inferior colliculus. Criteria were also developed for recognizing this same population of neurons in tissue that had been prepared under different histological conditions. Consequently, it was demonstrated that the group of midbrain-projecting neurons may be divided into at least two additional categories based on differences in dendritic morphology and location with respect to cortical layers. Our observations extended previous descriptions of the DCN from other strains of mice (e.g., C57BL/6J, Mugnaini et al., '80; CBA/J, Webster and Trune, '82) and are generally consistent with those of other nonprimate mammals including cat (e.g., Lorente de Nó, '81; Osen, '69; Kane, '74), guinea pig (Noda and Pirsig, '74), hamster (Schweitzer and Cant, '84), opossum (Willard and Martin, '83), and rabbit (Ramón y Cajal, '09; Disterhoft et al., '80; Perry and Webster, '81). In addition, the data generally agree with what has been reported for the cellular connections of the DCN (Beyerl, '78; Roth et al., '78; Adams, '79; Brunso-Bechtold et al., '81; Nordeen et al., '83; Trune, '83; Willard and Martin, '84; Zook and Casseday, '82). Finally, the structural features that characterize DCN organization are evident for albino (CD-1 and ICR) and pigmented (C57BL/6) strains of mice.

Midbrain-projecting neurons: The large, multipolar cells

One of the goals in this study was to identify the neurons in the DCN which projected to the IC. In the contralateral DCN, all large neurons were labelled following injections

TABLE 1. Distribution of Large Multipolar Neurons in the DCN

Animal	Strain	Technique	Number of neurons	Number of sections	Percentile	DCN Layers (%) I	II	III	IV
ICM-76	CD-1	HRP (large)	1,180	All (16)	All	0	78	18	4
ICM-77	CD-1	HRP (large)	656	All (15)	All	0	80	15	5
ICM-78	CD-1	HRP (large)	735	All (14)	All	0	77	17	6
MTK-53	ICR	Nissl	153	3	45, 50, 55	0	84	13	3
CN (n = 6)[1]	ICR	HRP (small)	301	All	All	0	73	21	6

[1]Data taken from Ryugo et al. ('81).

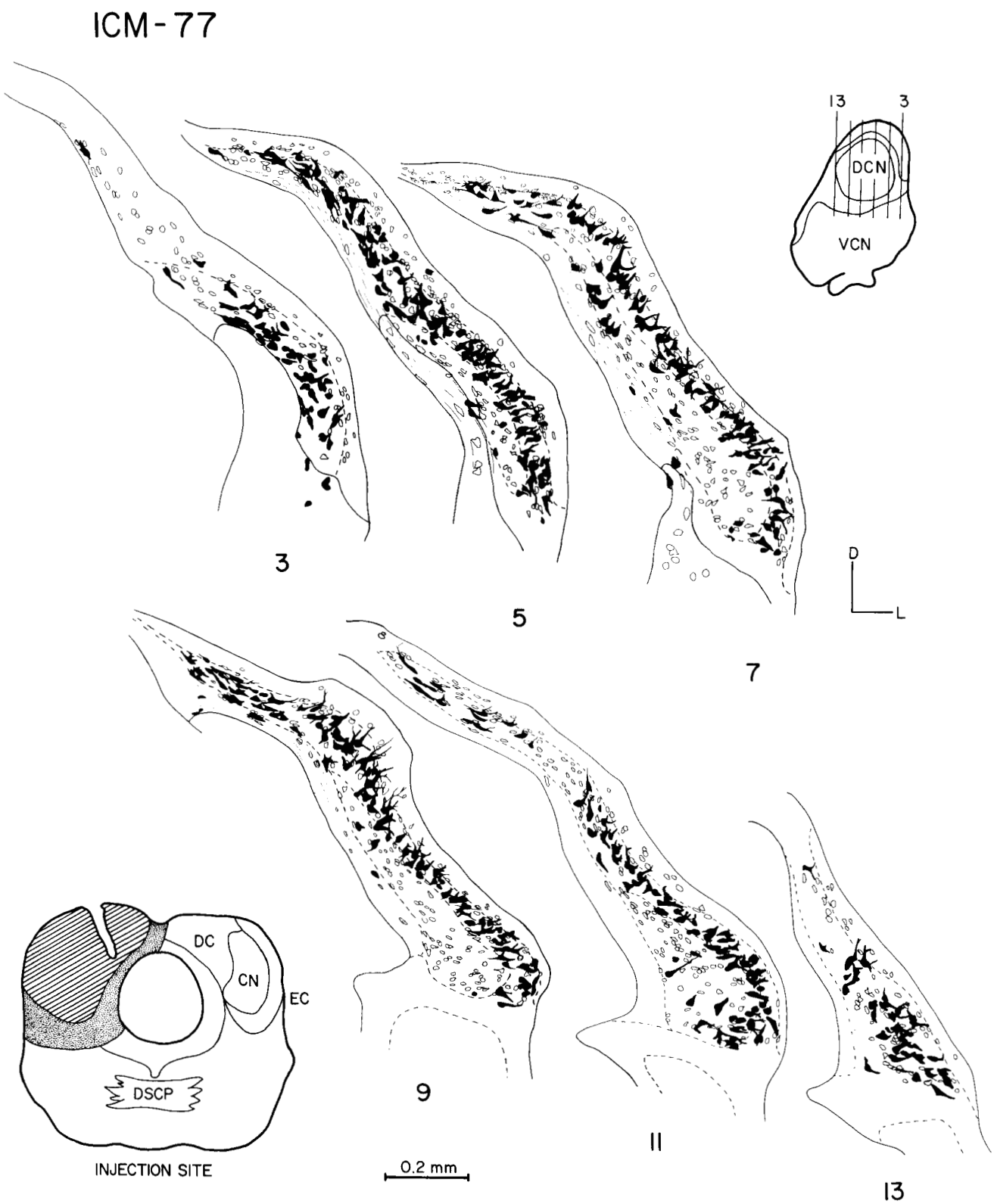

Fig. 8. Drawing tube reconstructions illustrating all labelled and unlabelled neurons in alternate sections through the contralateral DCN following an HRP injection into the inferior colliculus (see bottom inset for injection site and top inset for plane of section). Note that the labelled neurons tend to be the largest ones in the DCN and that they are located primarily in layer II. Abbreviations: CN, central nucleus of IC; DC, dorsal cortex of IC; EC, external cortex of IC; DSCP, decussation of superior cerebellar peduncle.

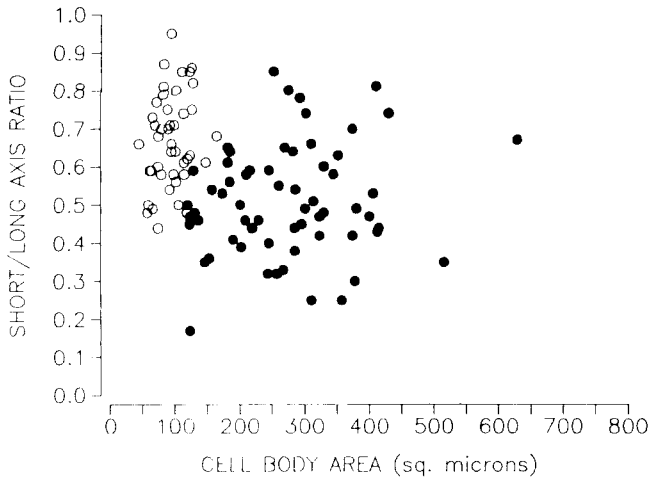

Fig. 9. Plot of cell body silhouette area and short/long axis ratio for all labelled (filled circles) and unlabelled (open circles) neurons in one 50-μm-thick coronal section through the 50th percentile of the nucleus (ICM-77). Note the general size separation between labelled and unlabelled neurons.

of the IC with solutions of HRP. In fact, only large neurons were labelled. Studies of the cat (Adams, '79) have described small neurons in the DCN that projected to the IC, but in our material, small labelled profiles were always found to represent parts of larger cells that were located in adjacent tissue sections. The previous observation that unlabelled large neurons were intermixed with labelled neurons of equal size (Ryugo et al., '81) must simply reflect inadequate access to HRP by some neurons due to the more restricted injections. At present, we cannot rule out the possibility that smaller cells also project to the IC but require some special treatment for their detection.

Our conclusion that all large neurons in the mouse DCN project to the contralateral IC is made in the light of previously reported data. In a preliminary study (Willard and Ryugo, '79), lesions of the dorsal acoustic stria (the output pathway of the DCN) were used to trace the trajectory and distribution of degenerating axons within the brainstem. It was noted that no axons of DCN origin projected rostral to the IC, which eliminated the interpretative problems of "fibers of passage" in the present study. Within the IC,

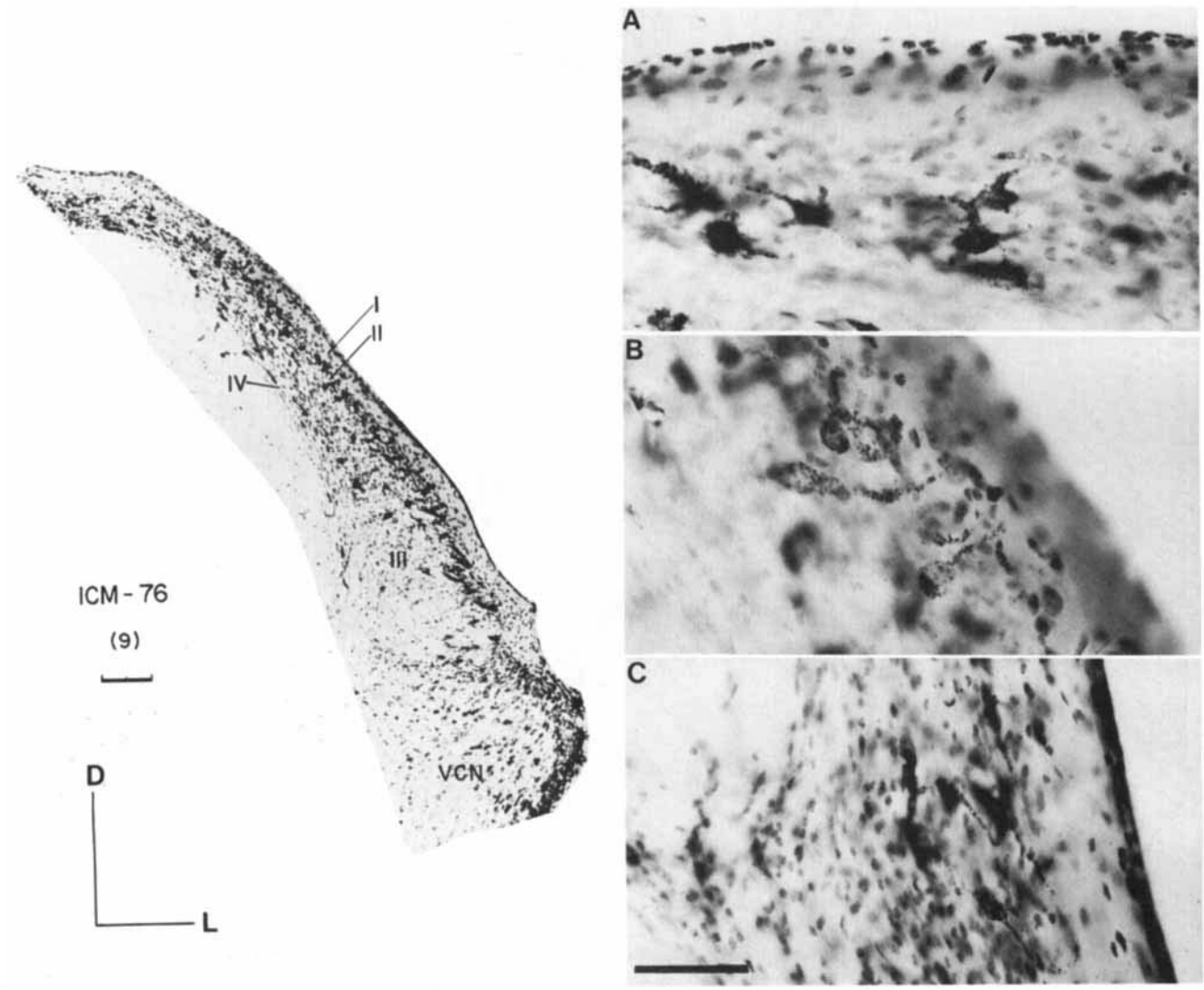

Fig. 10. Photomicrographs of HRP labelled neurons (ICM-76). Left, photomontage through the DCN illustrating orientation and shape changes of neurons as a function of position. Layers I–IV are indicated. Abbreviations: D, dorsal, L, lateral. Scale bar equals 0.1 mm. Higher-magnification photomicrographs of pyramidal cells taken from dorsomedial (A), central (B), and ventrolateral (C) positions in the DCN. Scale bar in panel C equals 50 μm.

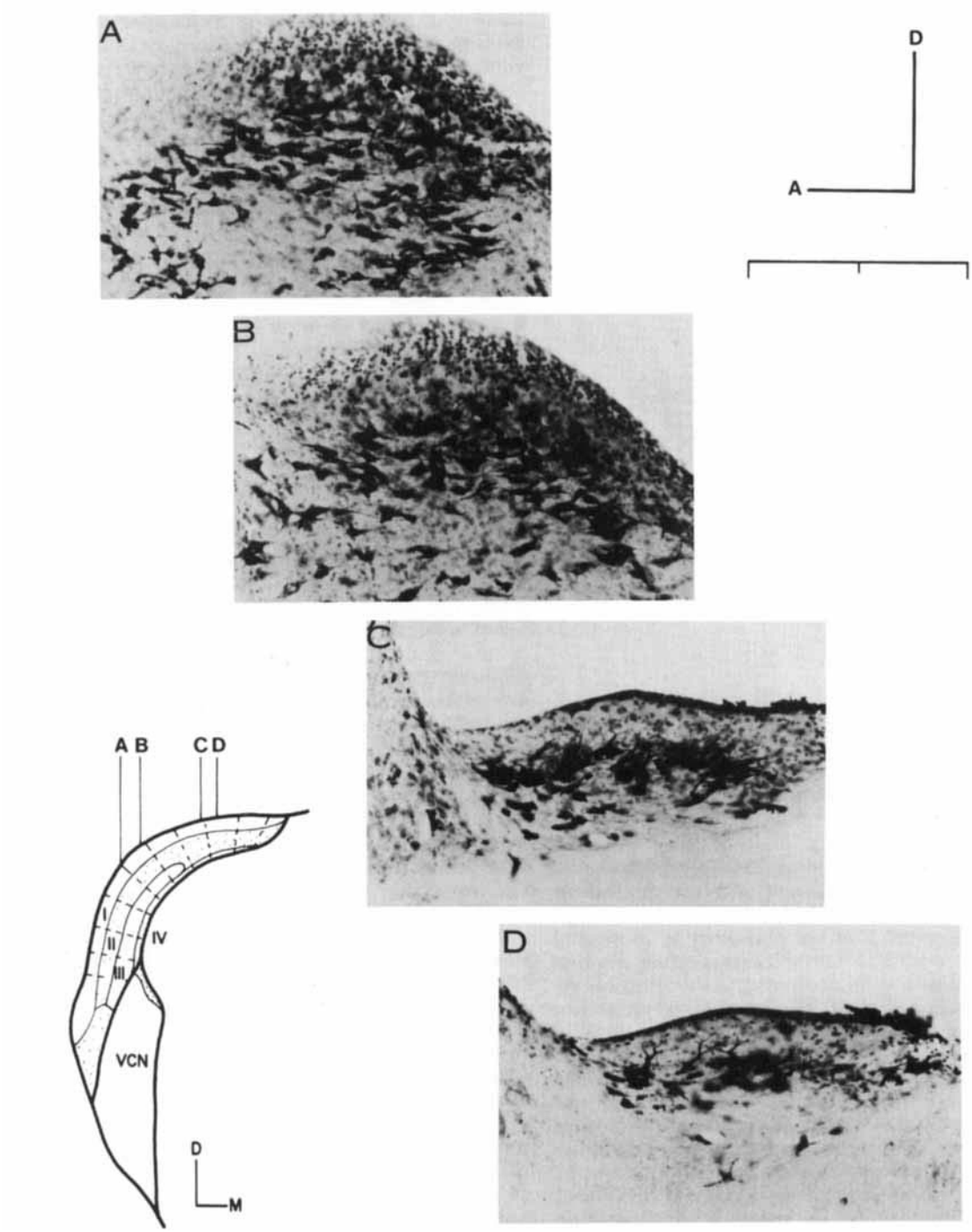

Fig. 11. Photomicrographs through representative parasagittal sections of the DCN following an HRP injection into the contralateral inferior colliculus (ICM-89). Most of the labelled neurons are located in layer II. Layer II is curved in photomicrographs A and B; it is relatively straight in C and D. The approximate position of each section within the nucleus is indicated by letter in the inset diagram. In the more lateral sections (A and B), labelled neurons are viewed "on edge;" in progressively more medial sections (C and D), the labelled neurons are viewed more en face. Adult CD-1 mouse. Scale bar equals 80 μm.

degenerating axons and preterminals were restricted to the central nucleus and external cortex and were not found in adjacent midbrain structures such as dorsal cortex of the IC, the periaqueductal gray, or the dorsal nucleus of the lateral lemniscus. Since the accumulation of extracellular HRP at the injection site did not spread beyond these structures in any of our present cases, we have concluded that the labelled neurons represent a unified population in the DCN that has a terminal field in the contralateral IC.

The IC, of course, is not the only target of DCN axons. Lesions of the dorsal acoustic stria revealed a strong projection to the ventral nucleus of the lateral lemniscus (VNLL) in addition to the IC (Willard and Ryugo, '83). These findings may be relevant to Osen's ('72) observations that sec-

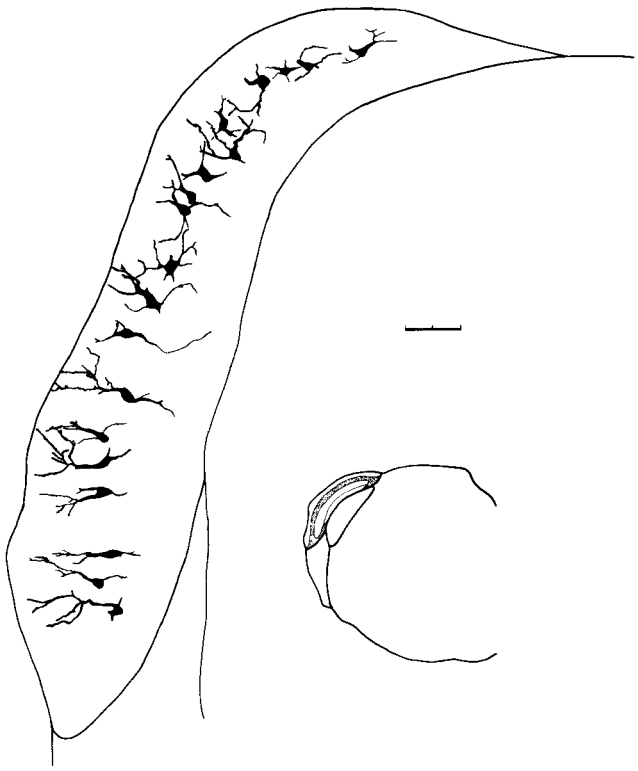

Fig. 12. Drawing tube reconstruction of all large neurons (cell body area greater than 250 μm^2) found in two consecutive coronal sections spanning the 50th percentile and located in layer II and the upper part of layer III. These pyramidal cells have relatively flattened dendritic fields. Note the progressive change in neuron orientation and dendritic length as a function of dorsomedial-to-ventrolateral position in the nucleus. Golgi-Kopsch, 60-day-old ICR mouse. Scale bar equals 0.1 mm.

tioning the lateral lemniscus immediately beneath the IC produces retrograde degeneration of all pyramidal cells in the DCN, and that giant cells remain essentially normal. It may be hypothesized that the projection by pyramidal cells to the IC is "essential" for their preservation, a notion originally articulated when describing thalamocortical relationships (Rose and Woolsey, '58). An essential projection, however, is not necessarily an exclusive projection, because intranuclear collaterals of pyramidal cells (Rhode et al., '83) could not prevent the retrograde degeneration. The giant cells that are spared from the retrograde degeneration are presumably preserved by "sustaining" collaterals that branch a healthy distance from the lesion and innervate the VNLL (and/or contralateral cochlear nucleus as described by Cant and Gaston, '82). Lesions in the dorsal acoustic stria would damage the essential and sustaining projections of efferent neurons of the DCN, producing the retrograde degeneration of both giant and pyramidal cells as reported by Osen ('72).

Cell body size emerges as a good predictor of a midbrain-projecting neuron, but it is not an absolute indicator since there is some size overlap (e.g., Figs. 7, 9). To a certain extent, the degree of size separation between the large multipolar neurons and other cells is diminished because some of the measured profiles represent only partial neurons due to the restricted thickness of the tissue sections, even though the "nuclear criterion" has been met. Such large multipolar neurons will therefore appear smaller. This intermixing may be further explained by variations in perikaryal shape of the large multipolar neurons at the extreme ends of the nucleus, especially in layer II. In the ventrolateral base of the DCN (corresponding to the tonotopically defined low frequency region), these neurons become quite elongated and the slender cell bodies have reduced silhouette areas. At the dorsomedial apex (high-frequency region), the DCN becomes markedly reduced in depth and there is a corresponding compression of principal cell bodies. These shorter cell bodies also exhibit smaller silhouette areas. It is rather striking, however, that the gradient in neuron height also follows the tonotopic organization of the nucleus. That is, neurons in the high-frequency region of the DCN exhibit the shortest dendrites, whereas neurons in lower-frequency regions exhibit progressively longer dendrites. The present observations in mice provide a more detailed context in which to interpret the classical illustrations from cat (Sala, 1893: Fig. 1) and rabbit (Ramón y Cajal, '09: Fig. 336). The relationship between dendritic length and frequency sensitivity is not well understood, but may be related to ontogenetic events in the nucleus (Smith and Rubel, '79).

Two types of large multipolar neurons

Descriptive criteria were established for identifying midbrain-projecting neurons in classical histological preparations. The diverse characteristics of these neurons were found to fall into two general neuron classes upon analysis of data obtained from separate specimens prepared under different conditions. In this manner, difficulties that can arise with the use of a single method are circumvented. At the light microscopic level, for example, both the HRP reaction product and Golgi precipitate obscure perikaryal Nissl patterns typical of the large multipolar neurons. Golgi methods, however, reveal dendritic arbors and HRP methods reveal axonal projections. Nevertheless, similarities in perikaryal cytology, size, and distribution among cortical layers are correlated with differences in dendritic morphology revealing two subcategories of large multipolar neurons.

One class of large multipolar cells resides primarily in layer II and the upper part of layer III. These neurons correspond to what others have called pyramidal cells (Sala, 1891, 1893; Mugnaini et al., '80; Osen, '69), bipolar cells (Lorente de Nó, '81), fusiform cells (Ramón y Cajal, '09; Brawer et al., '74; Kane, '74), or principal cells (Willard and Ryugo, '83). We have followed the suggestion by Blackstad et al., ('84) and adopted the term "pyramidal cell" in deference to Sala's (1891) early observations. Pyramidal cells represent an operationally described set of neurons that are highly similar to one another by virtue of a variety of shared morphological features. They have conspicuous Nissl bodies, pale-staining nuclei, and relatively flattened dendritic fields. Each dendritic field is compressed within the short axis dimension of the DCN and contributes to a fibrodendritic organization that lies parallel to the cellular laminae. This "anisotropic" feature is sufficiently characteristic that pyramidal cells can be recognized in several mammals including rodents (Willard and Ryugo, '81; Moore, '83; Schweitzer, '83) and cats (Blackstad et al., '84).

The other class of large multipolar neuron resides in the deeper regions of layer III and layer IV. These neurons appear homologous to what have previously been called giant cells (Osen, '69). They have cytological characteristics similar to the pyramidal cells but differ in dendritic structure: giant cells have relatively unbranched dendrites that

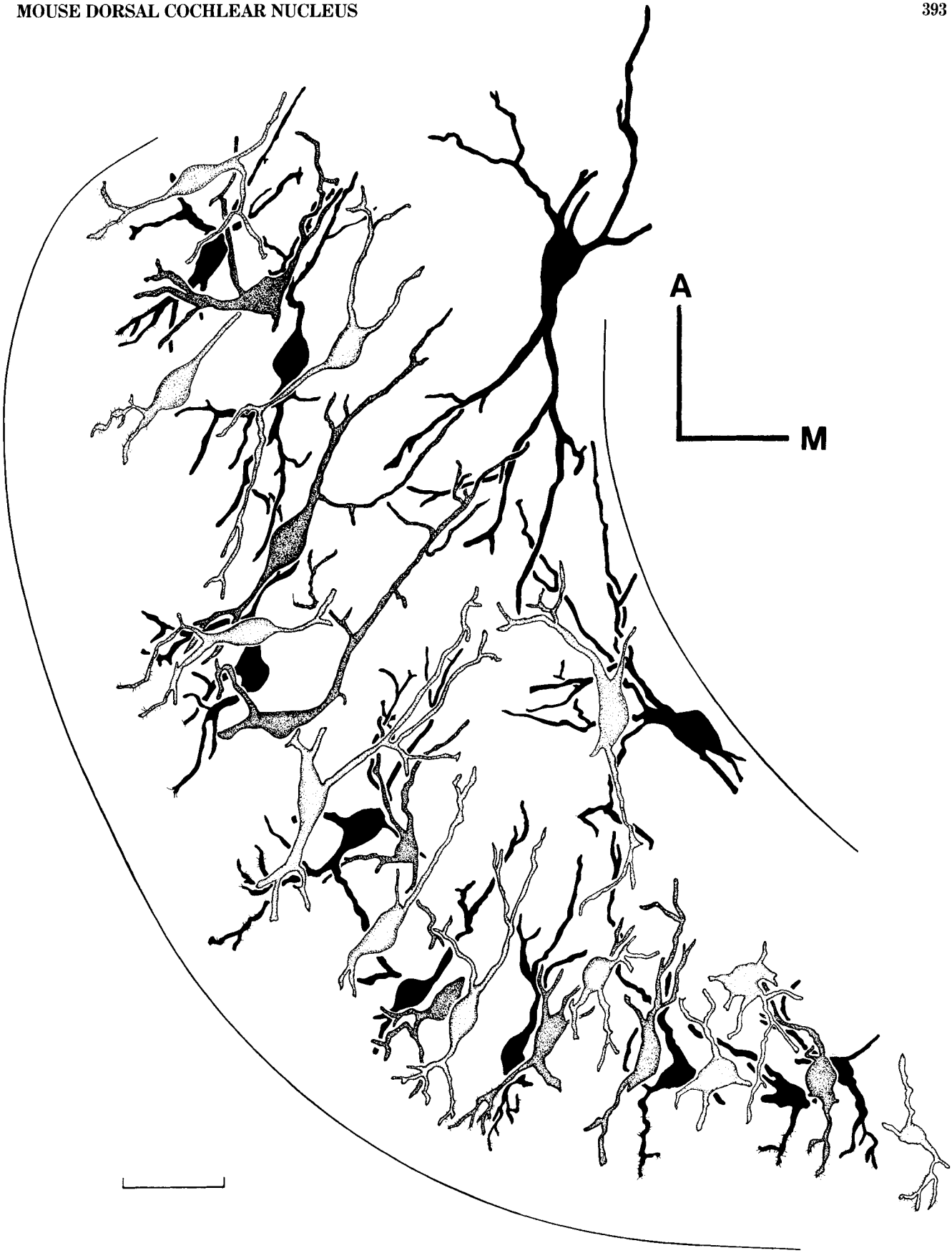

Fig. 13. Drawing tube reconstruction of all large neurons (cell body area greater than 250 μm^2) found in a single 100-μm-thick, horizontal section. Note how pyramidal cells, when viewed on edge, have a compressed dendritic field. The dendritic fields of deeper-lying giant cells (shown along the medial border of the nucleus) intersect a greater proportion of the DCN, and many of their distal dendrites appear aligned with basal dendrites of the pyramidal cells. Both cell types contribute to the formation of dendritic laminae. Golgi-Kopsch, 60-day-old CD-1 mouse. Scale bar equals 50 μm.

Fig. 14. Drawing tube reconstruction of three pyramidal cells from the DCN viewed *en face*. The dendritic fields are flattened and parallel to one another. These neurons radiate within the short axis dimension (plane of the page) but are compressed along the long axis (perpendicular to the page). Golgi-Kopsch, 60-day-old ICR mouse. Scale bar equals 20 μm.

form large, ellipsoidal arbors oriented along the long axis of the DCN.

It is acknowledged that in many respects the grouping of neurons into populations is contrived because we do not always know which characteristics have functional significance, and because group composition can change by altering membership criteria. For example, pyramidal cells are found in layers II and III and giant cells are found in layers III and IV. Alternatively, two types of pyramidal cells and two types of giant cells could be proposed by placing greater emphasis on position by layer. Using different criteria in cats, other categories of giant cells have also been suggested (Kane et al., '81). In any case, the nature of these hypothesized populations should be viewed in terms of the probable possession of a number of diverse features plus the absolute possession of a few.

Functional considerations

One prominent feature of many auditory structures in mammals is tonotopic organization (e.g., Clopton et al., '74). This physiological manifestation of frequency representation has been morphologically expressed in many (but not all) auditory regions as a pattern of repeating cell-and-fiber laminae that represent the acoustic frequency spectrum. As we have demonstrated, the DCN is no exception to this laminar pattern.

Orthogonal to the cortical layers of the DCN are parallel laminae derived from the alignment of the cell bodies in layers II and III and the planar dendritic fields of pyramidal cells. This laminar arrangement creates repeating sheets of neurons, and each sheet is innervated by auditory nerve fibers originating from a narrow sector of the cochlea. The bodies of both pyramidal and giant cells conform to this sheetlike arrangement. These neurons send their axons through the dorsal acoustic stria (Adams and Warr, '76), project in a topographical fashion to restricted laminae in the contralateral IC (Ryugo et al., '81), and exhibit type IV response properties (Young, '80). These laminae appear to be the morphological correlate to physiologically defined frequency bands (Mikaelian, '66; Willott, '83) and the conceptual equivalent to Lorente de Nó's ('81) "elemental slices."

The available electrophysiological evidence further suggests that individual pyramidal and giant cells conform to a frequency-selective (Godfrey et al., '75; Rhode et al., '83) and tonotopic organization of the nucleus (Rose et al., '59; Perry and Webster, '81). Since the dendritic arbors of pyramidal cells are confined to relatively narrow sectors of the DCN in contrast to those of the giant cells (which extend much more widely), it seems that the similarities in tuning characteristics of these separate cell types may be determined by different spatial patterns of primary inputs. Giant cells are hypothesized to receive most of their primary inputs on their cell bodies whereas pyramidal cells receive most of their primary inputs on their basal dendrites. Such a notion still awaits confirmation at the electron microscopic level.

It is also apparent that the dendritic arbors of the two neuron types are not entirely overlapping according to cortical layer. There is dendritic overlap only in layer III and perhaps the deeper region of layer II. Separation of dendritic fields occurs when the dendrites of pyramidal cells extend into layer I and the dendrites of giant cells extend into layer IV. Ultimately, the dendrites of the different cell

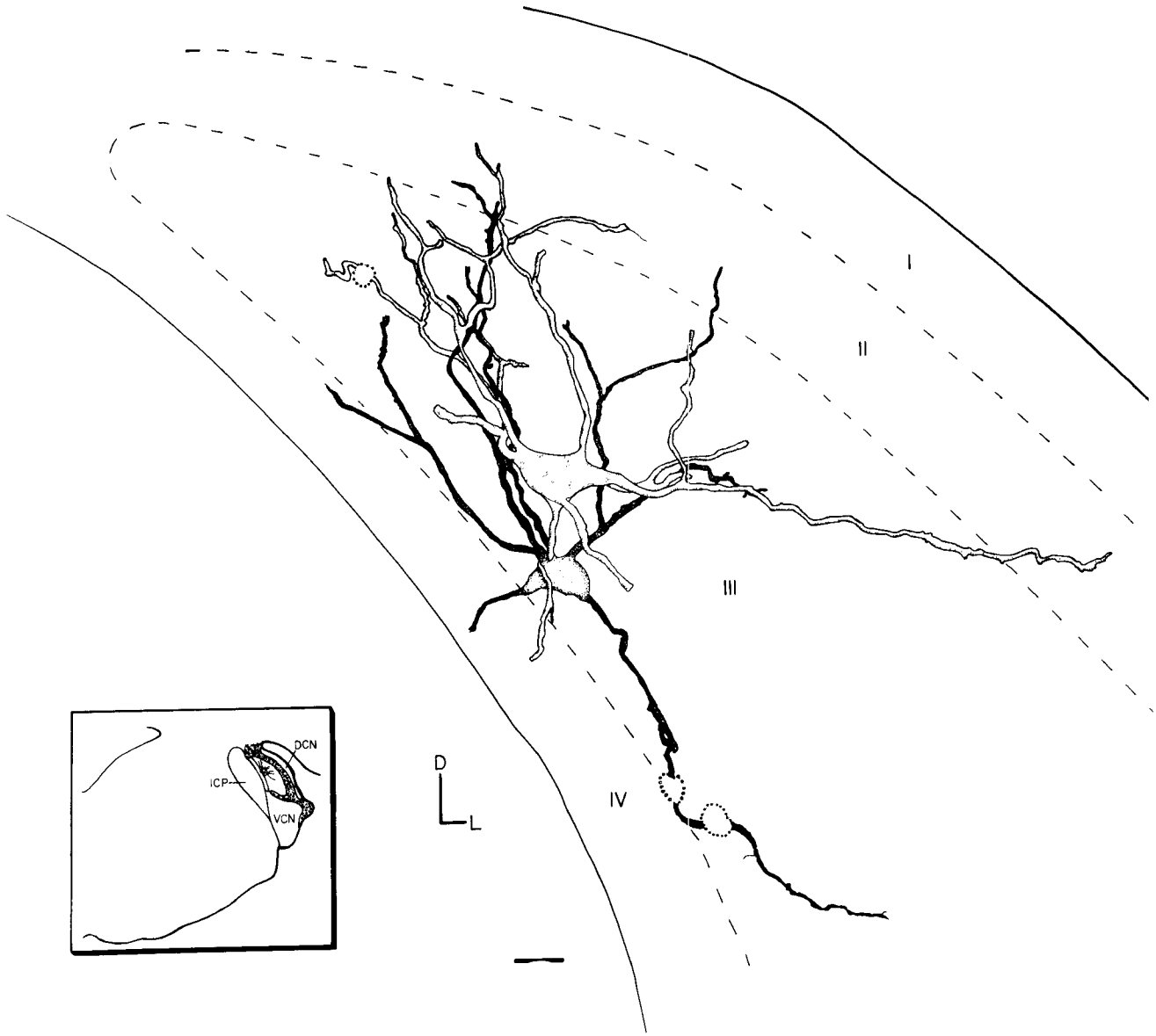

Fig. 15. Drawing tube reconstruction of two giant cells taken from layer III of the DCN (see inset for orientation). The dendritic fields are ellipsoidal and oriented along the long axis of the nucleus. Golgi-Kopsch, 60-day-old ICR mouse. Abbreviations are the same as in Figure 1. Scale bar equals 20 μm.

types can sample separate inputs to the DCN that are segregated according to cortical layer (e.g., Jones and Casseday, '79; Mugnaini et al., '80). On the basis of cell body position within the nucleus, these structural variations in the dendrites of the large multipolar neurons could correspond with the more subtle response variations reported for the physiologically defined type IV neurons (Young and Brownell, '76). The functional significance of these variations remains to be determined.

ACKNOWLEDGMENTS

The authors gratefully acknowledge the assistance of R. Cronin-Schreiber in the preparation of figures. We also thank T.E. Benson, A.M. Berglund, M.C. Brown, R. Cronin-Schreiber, D.M. Fekete, K.B. Henoch, T.N. Parks, M.R. Szpir, and E.H. Warren for their comments on an earlier draft of this manuscript. Computer programs for analysis were created by M.L. Curby, typing was performed by L. Dreesen and R.G. Vega, and photographic assistance was provided by H. Cook and P. Ley. Some of these results were presented in preliminary form at the 11th annual meeting of the Society for Neuroscience, Los Angeles, CA, 1981. This work was supported by NIH grants PO1 NS13126 and RO1 NS20156, and by the William F. Milton Fund of Harvard Medical School.

LITERATURE CITED

Adams, J.C. (1977) Technical considerations on the use of horseradish peroxidase as a neuronal marker. Neuroscience *2*:141–145.

Adams, J.C. (1979) Ascending projections to the inferior colliculus. J. Comp. Neurol. *183*:519–538.

Adams, J.C. (1983) Multipolar cells in the ventral cochlear nucleus project to the dorsal cochlear nucleus and the inferior colliculus. Neurosci. Lett. *37*:205–208.

Adams, J.C., and W.B. Warr (1976) Origins of axons in the cat's acoustic

striae determined by injection of horseradish peroxidase into severed tracts. J. Comp. Neurol. *170:*107–121.

Beyerl, B.D. (1978) Afferent projections to the central nucleus of the inferior colliculus in the rat. Brain Res. *145:*209–223.

Blackstad, T.W., K.K. Osen, and E. Mugnaini (1984) Pyramidal neurones of the dorsal cochlear nucleus: A Golgi and computer reconstruction study in cat. J. Neurosci. *13:*827–854.

Bodian, D. (1936) A new method for staining nerve fibers and nerve endings in mounted paraffin sections. Anat. Rec. *65:*89–95.

Brawer, J.R., D.K. Morest, and E.C. Kane (1974) The neuronal architecture of the cochlear nucleus of the cat. J. Comp. Neurol. *155:*251–300.

Brunso-Bechtold, J.K., G.C. Thompson, and R.B. Masterton (1981) HRP study of the organization of auditory afferents ascending to central nucleus of inferior colliculus in cat. J. Comp. Neurol. *197:*705–722.

Cant, N.B. (1982) Identification of cell types in the anteroventral cochlear nucleus that project to the inferior colliculus. Neurosci. Lett. *32:*241–246.

Cant, N.B., and K.C. Gaston (1982) Pathways connecting the right and left cochlear nuclei. J. Comp. Neurol. *212:*313–326.

Cant, N.B., and D.K. Morest (1984) The structural basis for stimulus coding in the cochlear nucleus of the cat. In C.I. Berlin (ed): Hearing Science: Recent Advances. San Diego: College-Hill Press, pp. 371–421.

Clopton, B.M., J.A. Winfield, and F.J. Flamino (1974) Tonotopic organization: Review and analysis. Brain Res. *76:*1–20.

Disterhoft, J.F., R.E. Perkins, and S. Evans (1980) Neuronal morphology of the rabbit cochlear nucleus. J. Comp. Neurol. *192:*687–702.

Fekete, D.M., E.M. Rouiller, M.C. Liberman, and D.K. Ryugo (1984) The central projections of intracellularly labelled auditory nerve fibers in cats. J. Comp. Neurol. *229:*432–450.

Godfrey, D.A., N.Y.-S. Kiang, and B.E. Norris (1975) Single unit activity in the dorsal cochlear nucleus of the cat. J. Comp. Neurol. *162:*269–284.

Harrison, J.M., and M.L. Feldman (1970) Anatomical aspects of the cochlear nucleus and superior olivary complex. In W.D. Neff (ed): Contributions to Sensory Physiology, Vol. 4. New York: Academic Press, pp. 95–142.

Jones, D.R., and J.H. Casseday (1979) Projections to laminae in dorsal cochlear nucleus in the tree shrew, *tupaia glis.* Brain Res. *160:*131–133.

Kane, E.C. (1974) Synaptic organization in the dorsal cochlear nucleus of the cat: A light and electron microscopic study. J. Comp. Neurol. *155:*301–331.

Kane, E.S., S.G. Puglisi, and B.S. Gordon (1981) Neuronal types in the deep dorsal cochlear nucleus of the cat: I. Giant neurons. J. Comp. Neurol. *198:*483–513.

Kiang, N.Y.S. (1975) Stimulus representation in the discharge patterns of auditory neurons. In D.B. Tower (ed): The Nervous System, Vol. 3: Human Communication and its Disorders. New York: Raven Press, pp. 81–96.

Lorente de Nó, R. (1981) The Primary Acoustic Nuclei. New York: Raven Press.

Mesulam, M.-M. (1976) The blue reaction product in horseradish peroxidase neurohistochemistry: incubation parameters and visibility. J. Histochem. Cytochem. *24:*1273–1280.

Mesulam, M.-M. (1978) Tetramethyl benzidine for horseradish peroxidase neurohistochemistry: A noncarcinogenic blue reaction-product with superior sensitivity for visualizing neural afferents and efferents. J. Histochem. Cytochem. *26:*106–117.

Mikaelian, D.O. (1966) Single unit study of the cochlear nucleus in the mouse. Acta. Otolaryngol. *62:*545–556.

Moore, J.K. (1983) Cytoarchitecture of the dorsal cochlear nucleus of the guinea pig. Assoc. Res. Otolaryngol. Abstr., 3.

Mugnaini, E., W.B. Warr, and K.K. Osen (1980) Distribution and light microscopic features of granule cells in the cochlear nuclei of cat, rat, and mouse. J. Comp. Neurol. *191:*581–606.

Noda, Y., and W. Pirsig (1974) Anatomical projection of the cochlea to the cochlear nuclei of the guinea pig. Arch. Oto-rhino-laryngol. *208:*107–120.

Nordeen, K.W., H.P. Killackey, and L.M. Kitzes (1983) Ascending auditory projections to the inferior colliculus in the adult gerbil, *meriones unguiculatus.* J. Comp. Neurol. *214:*131–143.

Osen, K.K. (1969) Cytoarchitecture of the cochlear nuclei in the cat. J. Comp. Neurol. *136:*453–484.

Osen, K.K. (1972) Projection of the cochlear nuclei on the inferior colliculus in the cat. J. Comp. Neurol. *144:*355–372

Perry, D.R., and W.R. Webster (1981) Neuronal organization of the rabbit cochlear nucleus: Some anatomical and electrophysiological observations. J. Comp. Neurol. *197:*623–638.

Ramón y Cajal, S. (1909) Histologie du Systeme Nerveux de l'Homme et des Vertebres, Vol. I. (1952 reprint). Madrid, Spain: Instituto Ramon y Cajal, pp. 754–838.

Rhode, W.S., P.H. Smith, and D. Oertel (1983) Physiological response properties of cells labeled intracellularly with horseradish peroxidase in cat dorsal cochlear nucleus. J. Comp. Neurol. *213:*426–447.

Rose, J.E., R. Galambos, and J.R. Hughes (1959) Microelectrode studies of the cochlear nuclei of the cat. Bull. Johns Hopkins Hospital *104:*211–251.

Rose, J.E., and C.N. Woolsey (1958) Cortical connections and functional organization of the thalamic auditory system of the cat. In H. Harlow and C.N. Woolsey (eds): Biological and Biochemical Bases of Behavior. Madison: University of Wisconsin Press, pp. 127–150.

Roth, G.L., L.M. Aitkin, R.A. Anderson, M.M. Merzenich (1978) Some features of the spatial organization of the central nucleus of the inferior colliculus of the cat. J. Comp. Neurol. *182:*661–680.

Ryugo, D.K., and D.M. Fekete (1982) Morphology of primary axosomatic endings in the anteroventral cochlear nucleus of the cat: A study of the endbulbs of Held. J. Comp. Neurol. *210:*239–257.

Ryugo, D.K., F.H. Willard, and D.M. Fekete (1981) Differential afferent projections to the inferior colliculus from the cochlear nucleus in the albino mouse. Brain Res. *210:*342–349.

Sala, L. (1891) Sur l'origine du nerf acoustique. Arch. Ital. Biol. *16:*196–207.

Sala, S. (1893) Ueber den Ursprung des Nervus acusticus. Arch. Mikrosk. Anat. *42:*18–52.

Schweitzer, L. (1983) The role of cochlear input in dendritic maturation in the dorsal cochlear nucleus of the hamster. Anat. Rec. *205:*178A–179A.

Schweitzer, L., and N.B. Cant (1984) Development of the cochlear innervation of the dorsal cochlear nucleus of the hamster. J. Comp. Neurol. *225:*228–243.

Smith, D.J., and E.W. Rubel (1979) Organization and development of brain stem auditory nuclei of the chicken: Dendritic gradients in nucleus laminaris. J. Comp. Neurol. *186:*213–240.

Tolbert, L.P., D.K. Morest, and D.A. Yurgelun-Todd (1982) The neuronal architecture of the anteroventral cochlear nucleus of the cat in the region of the cochlear nerve root: horseradish peroxidase labelling of identified cell types. Neuroscience *7:*3031–3052.

Trune, D.R. (1983) Influence of neonatal cochlear removal on the development of mouse cochlear nucleus. III. Its efferent projections to inferior colliculus. Dev. Brain Res. *9:*1–12.

Tsuchitani, C. (1978) Lower auditory brain stem structures of the cat. In R.F. Naunton and C. Fernandez (eds): Evoked Electrical Activity in the Auditory Nervous System. New York: Academic Press, pp. 373–401.

Webster, D.B., and D.R. Trune (1982) Cochlear nuclear complex of mice. Am. J. Anat. *163:*103–130.

Willard, F.H., and G.F. Martin (1983) The auditory brainstem nuclei and some of their projections to the inferior colliculus in the North American opossum. Neuroscience *4:*1203–1232.

Willard, F.H., and G.F. Martin (1984) Collateral innervation of the inferior colliculus in the North American opossum: A study using fluorescent markers in a double-labeling paradigm. Brain Res. *303:*171–182.

Willard, F.H., and D.K. Ryugo (1979) The external nucleus of the inferior colliculus: A site of overlap for ascending auditory and somatosensory projections in the mouse. Soc. Neurosci. Abstr. *5:*33.

Willard, F.H., and D.K. Ryugo (1981) The neuronal organization of the mouse dorsal cochlear nucleus. Soc. Neurosci. Abstr. *7:*55.

Willard, F.H., and D.K. Ryugo (1983) Anatomy of the central auditory system. In J.F. Willott (ed): The Auditory Psychobiology of the Mouse. Springfield, IL: Charles C. Thomas Publishers, pp. 201–304.

Willott, J.F. (1983) Central nervous system physiology. In J.F. Willott (ed): The Auditory Psychobiology of the Mouse. Springfield, IL: Charles C. Thomas Publishers, pp. 305–338.

Wouterlood, F.G., and E. Mugnaini (1984) Cartwheel neurons of the dorsal cochlear nucleus: A Golgi-electron microscopic study in rat. J. Comp. Neurol. *227:*136–157.

Young, E.D. (1980) Identification of response properties of ascending axons from dorsal cochlear nucleus. Brain Res. *200:*23–37.

Young, E.D., and W.E. Brownell (1976) Response to tones and noise of single cells in dorsal cochlear nucleus of unanesthetized cats. J. Neurophysiol. *39:*282–300.

Zook, J.M., and J.H. Casseday (1982) Origin of ascending projections to inferior colliculus in the mustache bat, *Pteronotus parnellii.* J. Comp. Neurol. *207:*14–28.